



Comparative Evaluation of Mn(II) Framework Substitution in MnAPSO-34 and Mn-impregnated SAPO-34 Molecular Sieves Studied by Electron Spin Resonance and Electron Spin Echo Modulation Spectroscopy

Gernho Back*, Yanghee Kim, Young-Soo Cho, Yong-Ill Lee¹ and Chul Wee Lee¹

Department of Chemistry, Changwon National University, Changwon 641-773, Korea

¹ Advanced chemical technology division, KRICT, Daejeon 305-606, Korea

Received April 23, 2002

Abstracts : MnAPSO-34 and Mn-impregnated SAPO-34(Mn-SAPO-34) sample were prepared with various manganese contents and studied by electron spin resonance(ESR) and electron spin echo modulation(ESEM). Electron spin echo modulation analysis of 0.07mol % Mn(relative to p) in MnAPSO-34 with adsorbed D₂O shows two deuteriums at 0.26 nm and two at 0.36 nm from Mn. This suggests that two waters hydrate an MnO₄ configuration with a D-O bond orientation for the waters as expect for a negatively charged site at low manganese content (0.1 mol%), the ESR spectra of MnAPSO-34 and MnH-SAPO-34 exhibit the same parameters($g \approx 2.01$ and $A \approx 89$ G), but the spectra obtained from MnAPSO-34 samples are better resolved. The decomposition temperature of as-synthesized MnAPSO-34 were in the range of 200 – 600 °C of the morpholine which is 12 °C higher than that in as-synthesized MnH-SAPO-34. Infrared spectra showed that the position of a band at 3450 cm⁻¹ shifted about 15 cm⁻¹ toward higher energy in MnAPSO-34 versus MnH-SAPO-34. The modulation depth of the two-pulse ESE of MnAPSO-34 with adsorbed D₂O is deeper than that of MnH-SAPO-34 with adsorbed D₂O. Three-pulse ESEM of MnAPSO-34 and MnH-SAPO-34 with adsorbed deuterium oxide shows that the local environments of manganese in the hydrated samples are different, suggesting that Mn(II) is framework substituted in MnAPSO-34 since it obviously occupies an extraframework position in MnH-SAPO-34.

INTRODUCTION

Microporus crystalline aluminophosphates(AIPO₄-n) have been recently synthesized hydrothermally with morpholine being used as the templating agent.¹⁻³ Isomorphous substitution of several different element into the AIPO₄-n framework can be possible, of

* To whom : ghback@sarim.changwon.ac.kr

which the framework phosphorus substitution by silicon is of particular importance for their application such as adsorbents for separation and purification of molecular species, catalysts, or catalyst supports, and ion-exchange agents.⁴

Several research groups have characterized Mn(II) ions in various $\text{AlPO}_4\text{-n}$ and SAPO-n structures. It is reported that Mn(II) ions occupy framework positions in $\text{AlPO}_4\text{-11}$ ⁵ and SAPO-11⁶, while attempts of incorporated Mn(II) ions into lattice positions of $\text{AlPO}_4\text{-5}$ ^{7,8} have been unsuccessful. Both SAPO-11/ $\text{AlPO}_4\text{-11}$ and $\text{AlPO}_4\text{-5}$ have received a majority of attention because of their novel type structures. SAPO-34 is a silicoaluminophosphate which is structurally related to the naturally occurring silicoalumininate, chabazite. Currently Ni(II)⁹ and Co(II)^{10,11} have been reported to occupy lattice positions in SAPO-34. However, there are no reports describing the synthesis or characterization of Mn(II) ions in framework positions of SAPO-34.

In this report we present ESR and ESEM data on MnAPSO-34. ESR was used to monitor the changes in the hydration of the Mn(II) species after various thermal treatments while deuterium modulation from the ESEM data was also used for determining the number of water molecules coordinated to Mn(II) cation. These results were compared to those obtained by exchanging Mn(II) ions into extra-framework positions of H-SAPO-34. The comparison of the ESR and ESEM data for MnAPSO-34 versus MnH-SAPO-34 can be aided in determining whether Mn(II) ions can be incorporated into the SAPO-34.

EXPERIMENTAL

Syntheses and Sample Treatment

MnAPSO-34 was prepared by modifying the $\text{H}_2\text{O-HF}$ synthesis route described by Xu et al.¹² This method proved to be successful for synthesis of SAPO-34 and described well in the literature.¹³ An aqueous solution (2.96 ml) of H_3PO_4 (Mallinckrodt) was prepared by diluting the solution with 5 ml of de-ionized water and stirred for 10 min. After adding 5 ml of de-ionized water to the H_3PO_4 solution with continuous stirring, four portion (0.729 g for each time) of 2.915 g of $\text{Al}_2\text{O}_3\cdot\text{H}_2\text{O}$ (Vista Chemical B) were added successively every hour. The resulting homogeneous mixture was followed by adding of 0.32 g of fumed SiO_2 (Cab-O-Sil total 0.72 g fumed SiO_2) every 30 min over 2 h periods. Then, the mixture was cooled in ice water and 3.52 g of morpholine (Aldrich) and 2.5 ml of de-ionized water were added dropwise followed by continuous stirring at room temperature. The solution was stirred overnight and Mn(II) ions are introduced into the reaction mixture by means of manganese acetate solution[0.012 g of $\text{Mn}(\text{Acetate})_2$ in 2.5 ml of de-ionized water]. After the adding of Mn(II) ions, the reaction mixture was stirred for four hours to ensure the homogeneous distribution of Mn(II) ions. Various MnAPSO-34 samples were prepared with 0.07 mol% of manganese $\{(\text{Mn}/\text{Mn} + \text{Al} + \text{Si} + \text{P})\times 100\}$. A teflon-lined autoclave was filled to 50 % of its capacity with synthetic mixture and heated to 200°C and kept for 48 hours. The autoclave was then quenched with cold water

and the top liquid portion was removed with a pipette followed by washing the crystallized solid product three times with 250 ml of boiling de-ionized water. Finally the solid product was dried at 110 °C for 12 h in air. This as-synthesized MnAPSO-34 was analyzed by electron probe microanalysis MnAPSO-34 had a molar composition of 0.07 mol%. Comparison of the literature X-ray diffraction pattern with that of the synthesized product showed that the product was single phase with good crystallinity as shown in Fig. 1. MnAPSO-34 with 0.01 mol% manganese (100 Mn/Mn + Al + P + Si) was also prepared by the above same synthetic procedure of the MnAPSO-34 with 0.07 mol% manganese.

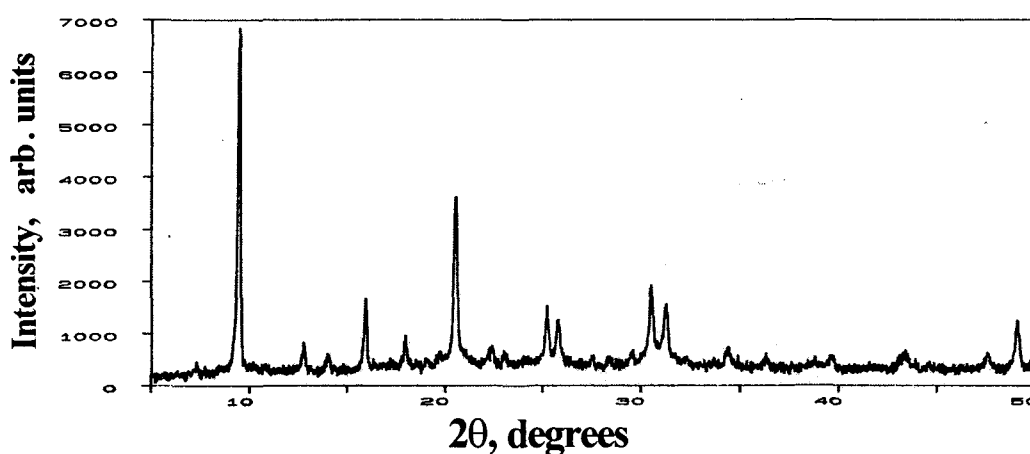


Fig. 1. X-ray powder diffraction pattern of as-synthesized MnAPSO-34.

Synthesis of SAPO-34 were carried out by a modification of the reported methods in the literature.¹² An aqueous solution (4.5 ml) of 85 % H_3PO_4 (Mallinckrodt) was prepared by diluting the solution with 6.7 ml of de-ionized water and stirred for 10 min. After adding 7.7 ml of de-ionized water to the H_3PO_4 solution with continuous stirring, four portions (0.175 g for each time) of 0.7 g of $Al_2O_3 \cdot H_2O$ (Vista Chemical B) were added successively every hour. The resulting homogeneous mixture was followed by successive addition of 0.20 g of fumed SiO_2 (Cab-O-Sil total 0.8 g fumed SiO_2) every 30 min over 2 h periods. Then, the mixture was cooled in ice water and 13.9 ml of triethylamine (Aldrich) was added dropwise followed by continuous stirring at room temperature. The solution was stirred overnight to give a bulk mole ratio of $Si_1Al_3P_5$. After about 14 h of stirring, the pH of the mixture was adjusted to 6.9 by the addition of 40 wt% HF solution (Aldrich). A Teflon-lined autoclave was filled to 50 % of its capacity with the synthesis mixture and heated to 200 °C and kept for 6 days. The autoclave was then quenched with cold water and the top liquid portion was removed with a pipette followed by washing the crystallized solid product three times with 250 ml of boiling deionized water. Finally the solid product was dried at 110 °C for 12 h in air. This as-

synthesized SAPO-34 was analyzed by electron probe microanalysis and had a molar composition of $\text{Si}_{0.11}\text{Al}_{0.55}\text{P}_{0.34}$. Comparison of the literature X-ray diffraction pattern with that of the synthesized product showed that the product was single phase with good crystallinity.

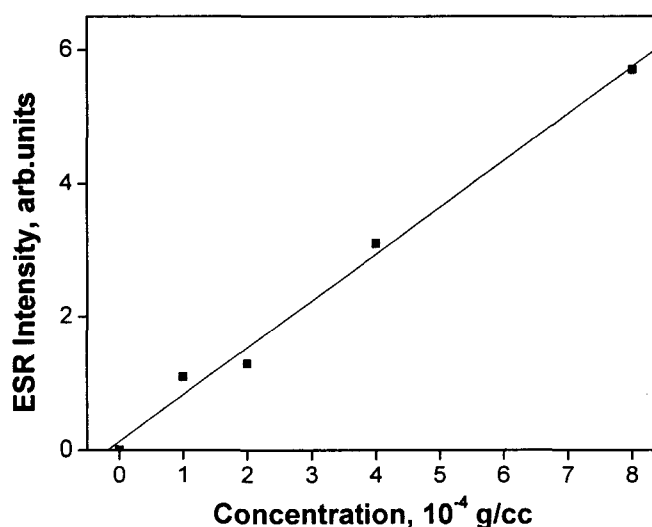


Fig. 2. Calibration curve of Mn(II) ion by double integration of ESR spectrum.

Sample ion-exchanged in the liquid phase and denoted by MnH-SAPO-34 was prepared by adding 10 ml of 1×10^{-1} M MnCl_2 in methanol media to 0.1 g of calcined H-SAPO-34 followed by stirring at 80°C for 2 h. The ion-exchanged product was then filtered, washed with 20 ml of methanol three times and dried in vacuum desiccator at room temperature for 15 h. The product was ground with a mortar and pestle and pressed in a steel die with about 2 tons for 20 min to make wafers of 12-mm diameter and 2.5-thickness. Then pellet was put in a quartz boat and heated in a furnace at 600°C in O_2 and kept for 15 h. The sample before and after the ion-exchanged reaction was white. Since this templating-free MnH-SAPO-34 loses its crystallinity slowly with moisture, the sample were stored under vacuum. The concentration of manganese was measured for the MnH-SAPO-34 from a calibration curve of the standardized MnCl_2 solution (See Fig. 2). This method is based on the measurement of the quantity of manganese adsorbed on a solid surface for SAPO-34 molecular by sensing the change in intensity of EPR spectrum obtained by double integration. It was found to be 0.01 mol% for the as-synthesized sample. To examine the change in the Mn(II) ion concentration as a function of hydration

environment, the sample is heated under vacuum to a residual pressure of about 10^{-4} torr. Prior to ESR and ESEM measurements the organic template was removed from the as-synthesized samples by heating to 600 °C in flowing oxygen, the temperature being raised slowly over an eight hours period then held at 600 °C overnight.

For comparison purpose Mn(II) ions were doped into a template free sample of H-SAPO-34. Due to the sensitivity of calcined SAPO-34 to moisture methanol is used as the exchange medium. The cocentration of Mn(II) ions, assuming complete exchange, is about 0.7 mol%. From the low resolution of the ESR and ESEM signals it is apparent that the amount of Mn(II) ions exchanged is less than 0.7 mol%. Samples ion-exchanged in the liquid phase (L) and denoted by (L)MnH-SAPO-34 were prepared by adding 50 ml of 1.32×10^{-3} M MnCl_2 (Aldrich) in methanol to 0.4343 g of calcined H-SAPO-34 followed by stirring at 80 °C for 2 h. The sample was then filtered, washed with hot (about 70 °C) methanol three times and dried in dry oven at 100 °C. The MnH-SAPO-34 sample was white and X-ray analysis gave 0.07 atom% of Mn relative to all T atoms.

Samples for ESEM experiments were pretreated by evacuation at 550 °C overnight and equilibration with D_2O at room temperature for 30 min before sealing in Suprasil quartz tubes with sample end immersed in liquid nitrogen.

Measurement

The synthetic molecular sieves were examined by powder X-ray diffraction (XRD) with a Phillips PW 1840 diffractometer. Thermogravimetric measurements were performed using a Universal V3.2B thermal analyzer (heating rate 5 °C/min). Infrared spectra were obtained with a Nicolet Impact 410 FT-IR spectrophotometer by the KBR pellet method. X-band ESR spectra were recorded at 77 K with a Varian E-4 spectrometer. The Microwave frequency were measured by a Hewlett-Packard HP 5342A frequency counter. ESEM spectra were measured at 4 K on a Bruker ESP 380 pulsed ESR spectrometer described elsewhere.¹⁴ Two- and three-pulse echoes were recorded by using 90° - τ - 180° and 90° - τ - 90° - T - 90° pulse sequences, where the echo is measured as a function of τ and T , respectively. Calcined MnAPSO-34 had 0.07 atom% Mn relative to all T atoms(Mn + Si + Al + P) by electron probe microanalysis with JEOL JXA-8600 spectrometer. The ESEM data are transferred to a Samsung 686 IBM PC compatible computer for data analysis. Simulation of the deuterium modulation observed is perfomed using the analytical expressions derived by Dikanov et al.¹⁵ Data are extracted from the modulation pattern by comparing the experimental ESEM signal with the calculated signal. The best fit is found by varying the parameter; the number of interesting nuclei, N , the interacting distance R and the isotropic hyperfine interaction A_{iso} , until sum of the square residuals is minimized.

RESULTS AND DISCUSSION

There are no significant differences in the XRD patterns between as-synthesized MnAPSO-34 and as-synthesized SAPO-34. This indicates that MnAPSO-34 has the same framework structure as SAPO-34. It is not easy to determine the presence of SAPO-34 and chabazite phases from the MnH-SAPO-34 because the XRD patterns of SAPO-34, chabazite zeolite, MnAPSO, and MnH-SAPO-34 are expected to be almost the same. From the comparison of the XRD patterns of SAPO-34 synthesized according to the literature with that of MnAPSO-34, no peak broadening was seen. Thus it is not surprising that the XRD does not give clear information on possible multiple phases present. When Mn(II) is added during synthesis to form MnAPSO-34 samples where the concentration of Mn(II) ions exceeded 0.05 mol%, no color change was observed after dehydrated samples are exposed to water vapor. The absence of a color change from purple to pale violet indicates that the restoration of the hydrated Mn(II) species does not occur. Regeneration of the hydrated Mn(II) species was achieved only after a sample evacuated at room temperature was exposed to water vapor. However, when Mn(II) was incorporated by liquid ion-exchanged to form MnH-SAPO-34, the product was white. This color difference indicates the different sites for Mn(II) in the synthesized and ion-exchanged materials. There is a significant color difference, depending on the position of Co(II) which is a tetrahedral framework or ion-exchanged site in CoAPO-5.¹⁷

Electron Spin resonance : Fig. 3 and 4 show the X-band ESR spectra of MnAPSO-34 samples with 0.07 and 0.01mol% Mn(II) ions after various thermal treatments. For comparison, the X-band ESR spectra after various dehydration steps for H-SAPO-34 exchanged with Mn(II) ions, where the Mn(II) ions are in the extra-framework positions, are illustrated in Fig. 5 and 6. All signals show six hyperfine lines which correspond to the $\Delta M_s = \pm 1/2$ transition. Shoulders between the six hyperfine lines are apparent in all the ESR signals with the exception of dehydrated MnH-SAPO-34. The appearance of shoulders can be attributed to either a second Mn(II) species or forbidden transitions ($\Delta M_s = \pm 1$) according to previous Mn(II) ESR studies.¹⁶

For all samples calcined, hydrated and dehydrated did not change the g value but does generate a slight alteration in the hyperfine coupling constant. After calcinations of the MnAPSO-34 samples the hyperfine coupling constant was increased from 83 G to 87 G as shown in Table 1. An increase in the hyperfine coupling constant was also observed in MnAPSO-11, while MnAPSO-44 was reported to have a more drastic reduction in this value after dehydration.¹⁷

Some distinct features observed in the ESR signals of MnH-SAPO-34 and MnAPSO-34 during the dehydration processes are (1) for all two samples a decrease in the A value of

about 7 G is noted; dehydration 400 °C of MnH-SAPO-34 results in a decrease in the intensity of the ESR signal by a factor of 10, the superimposition of a background signal is observed and the shoulders present in hydrated samples disappear; (2) 0.07 mol% MnAPSO-34 dehydrated at 100 °C the ESR signal is broadened and the hyperfines disappear, with further dehydration (400 °C) weak hyperfine splittings are observed.

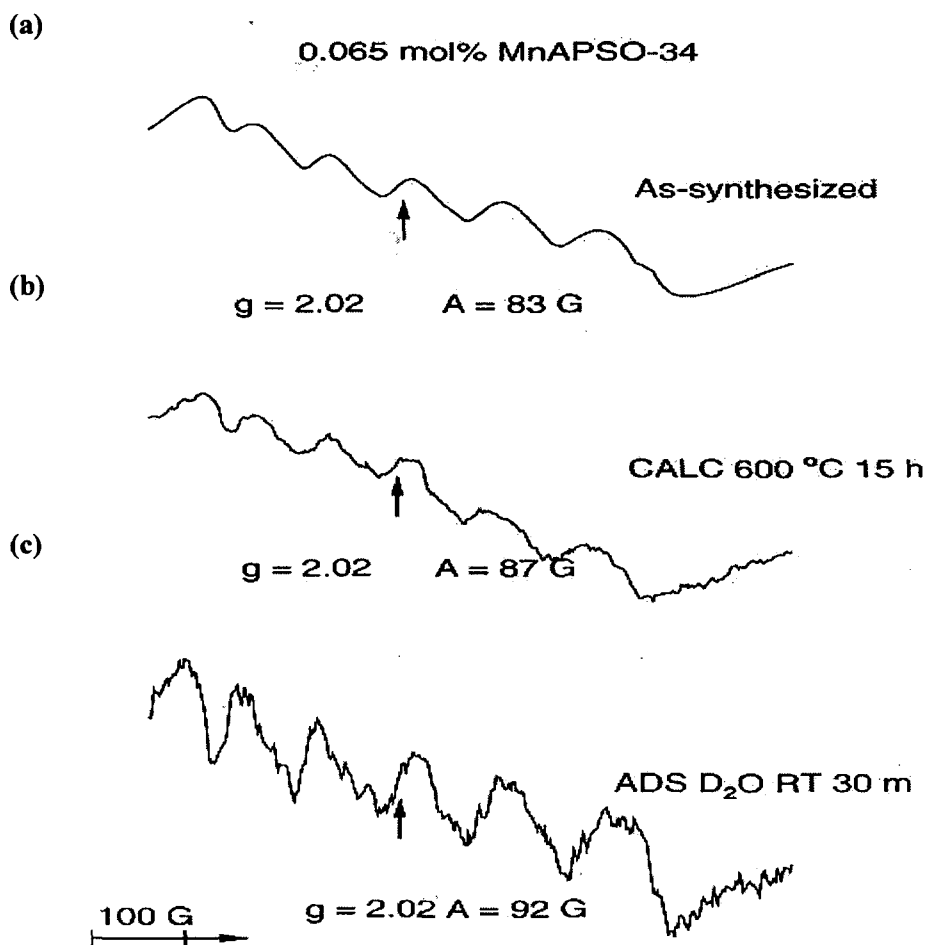


Fig. 3. ESR spectra recorded at 77 K of (a) as-synthesized MnAPSO-34 with 0.065 mol% manganese and (b) MnAPSO-34 with 0.065 mol% manganese calcined at 600 °C for 15 h and (c) calcined MnAPSO-34 with 0.065 mol% manganese adsorbed at room temperature for 30 min.

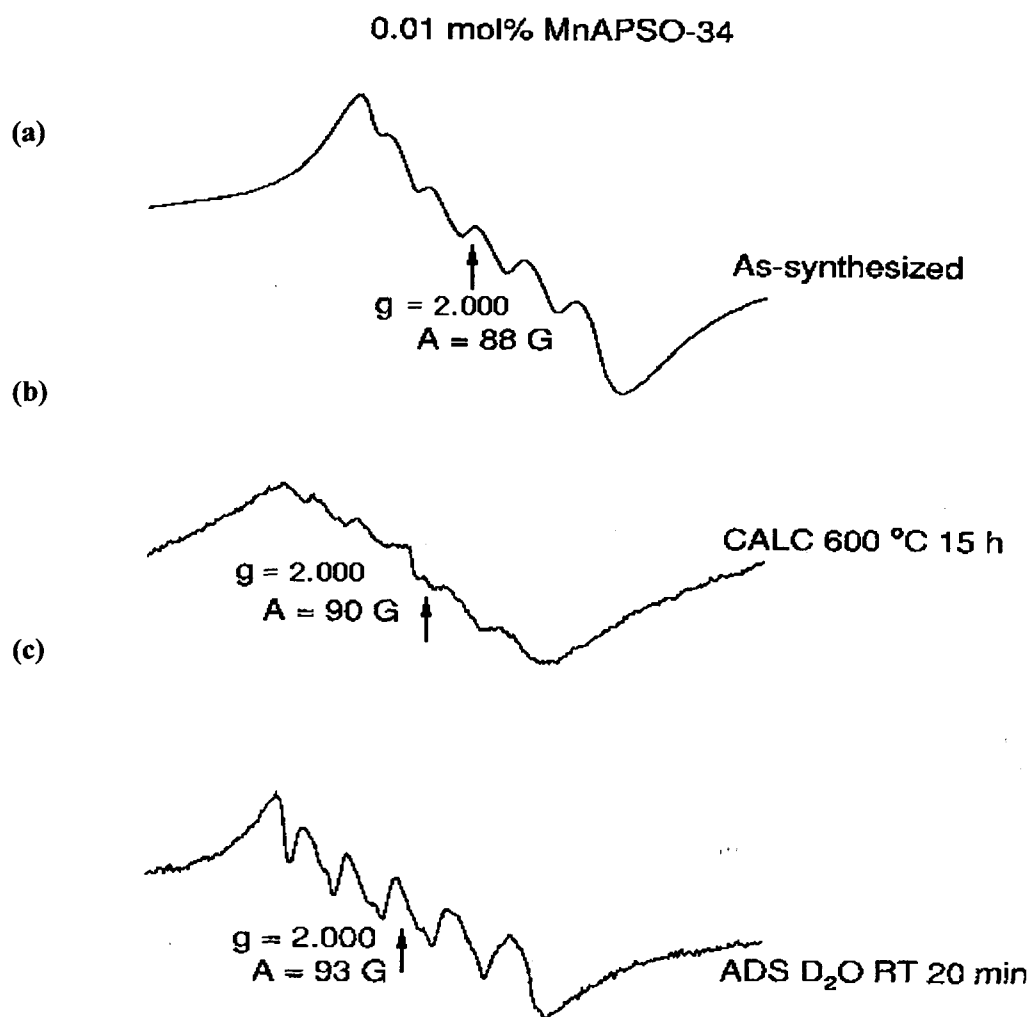


Fig. 4. ESR spectra recorded at 77 K (a) as-synthesized MnAPSO-34 with 0.01 mol% manganese and (b) MnAPSO-34 with 0.01 mol% manganese calcined at 600 °C for 15 h and (c) calcined MnAPSO-34 with 0.01 mol% manganese adsorbed D₂O at room temperature for 20 min.

Table 1. ESR Parameters of Mn(II) in MnAPSO-34 and MnH-SAPO-34.

Sample	g	hyperfine splitting, G
MnAPSO-34 as-synthesized	2.02	83
MnAPSO-34 calcined ^a	2.02	87
MnAPSO-34 hydrated ^b	2.02	89
MnH-SAPO-34 as-synthesized	2.02	83

^aat 600 °C for 15h.

^bafter calcinations followed exposure of air at room temperature for 15 h.

The broadening of the ESR signal implies that the Mn(II) ions are no longer isolated from one another. A similar type of ESR signal broadening is reported for Mn-APO-11 where the Mn(II) ions are found to occupy extra-framework positions.¹⁶ This indicates that the increase of spin-spin interaction is occurred some aggregation of the Mn(II) ions due to a decrease in the distance between the Mn(II) ions upon dehydration.

Thermogravimetric Analysis. The TGA curves of as-synthesized SAPO-34 and as-synthesized MnAPSO-34 are shown in Fig. 7. The weight loss observed between 25 and 280 °C is 5.0 % and that between 280 and 650 °C is 15 % for the amount of water and organic molecules, respectively. This is caused by the adsorption of water and a high temperature exothermic attribute to the desorption and decomposition of the organic molecule of TA profiles.¹⁸ Four stages of weight loss at ~90, ~279, ~400, and ~610 °C were clearly observed. The first and the second stage of weight loss were due to the desorption of water physically or chemically adsorbed on SAPO-34 and MnAPSO-34. The other losses except 279 °C are probably due to the decomposition of the organic templating agent, morpholine. While the temperature of the second loss was appeared for only MnAPSO-34, the temperature of the third and fourth losses for the as-synthesized MnAPSO were higher than the as-synthesized SAPO-34 by $\cong 10$ °C. The desorption near 280 °C are assigned to the water adsorbed chemically on Mn(II) and the desorptions near 400-600 °C are assigned to the protonated morpholine, which indicates the presence of acid sites. The higher decomposition temperature for as-synthesized MnAPSO-34 indicates that the Mn(II) in MnAPSO-34 has a different local electronic environment than does Mn(II) in ion-exchanged MnH-SAPO-34.

Infrared Spectra. Further evidence on the difference in the substitution of Mn(II) for the synthesized and ion-exchanged samples can be obtained from the infrared spectra in the frequency region 4000-3000 cm^{-1} (Fig. 8).

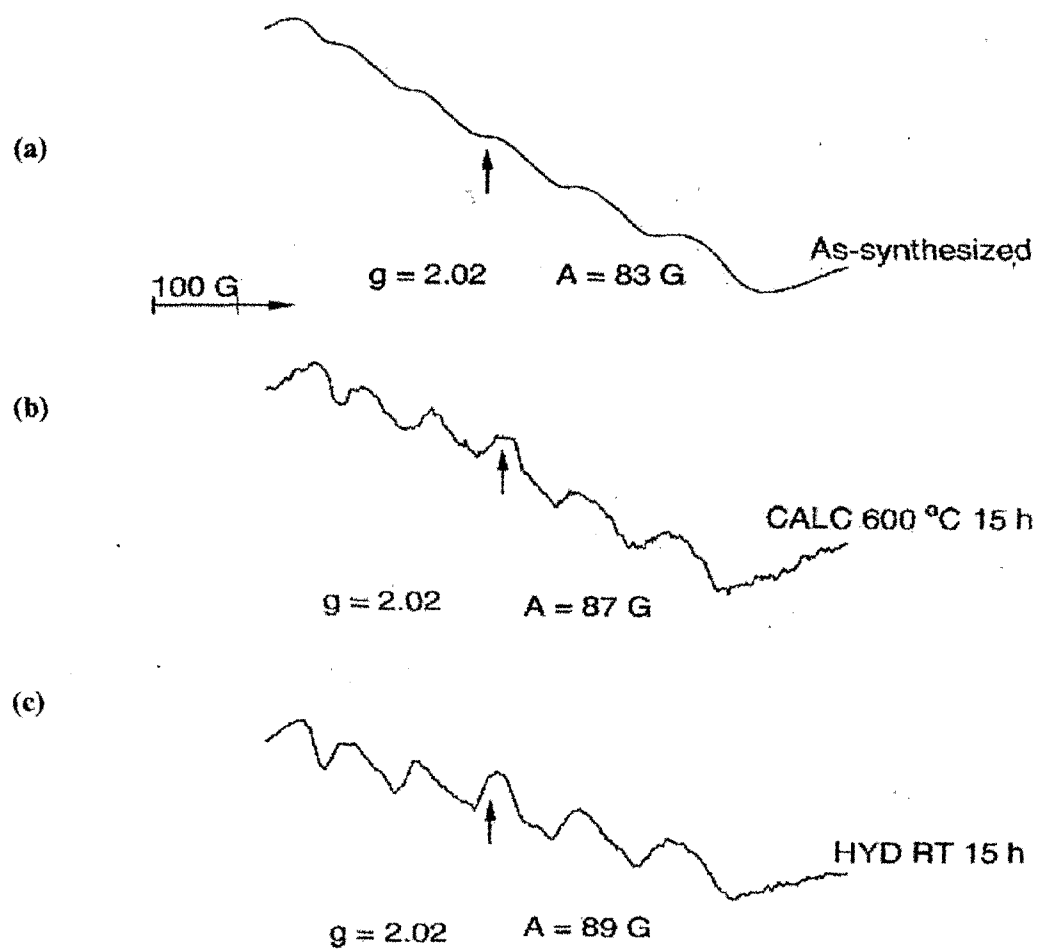


Fig. 5. ESR spectra recorded at 77 K (a) as-synthesized MnH-SAPO-34 with 0.065 mol% manganese and (b) MnH-SAPO-34 with 0.065 mol% manganese calcined at 600 °C for 15 h and (c) calcined MnH-SAPO-34 with 0.065 mol% manganese adsorbed air at room temperature for 15 h.

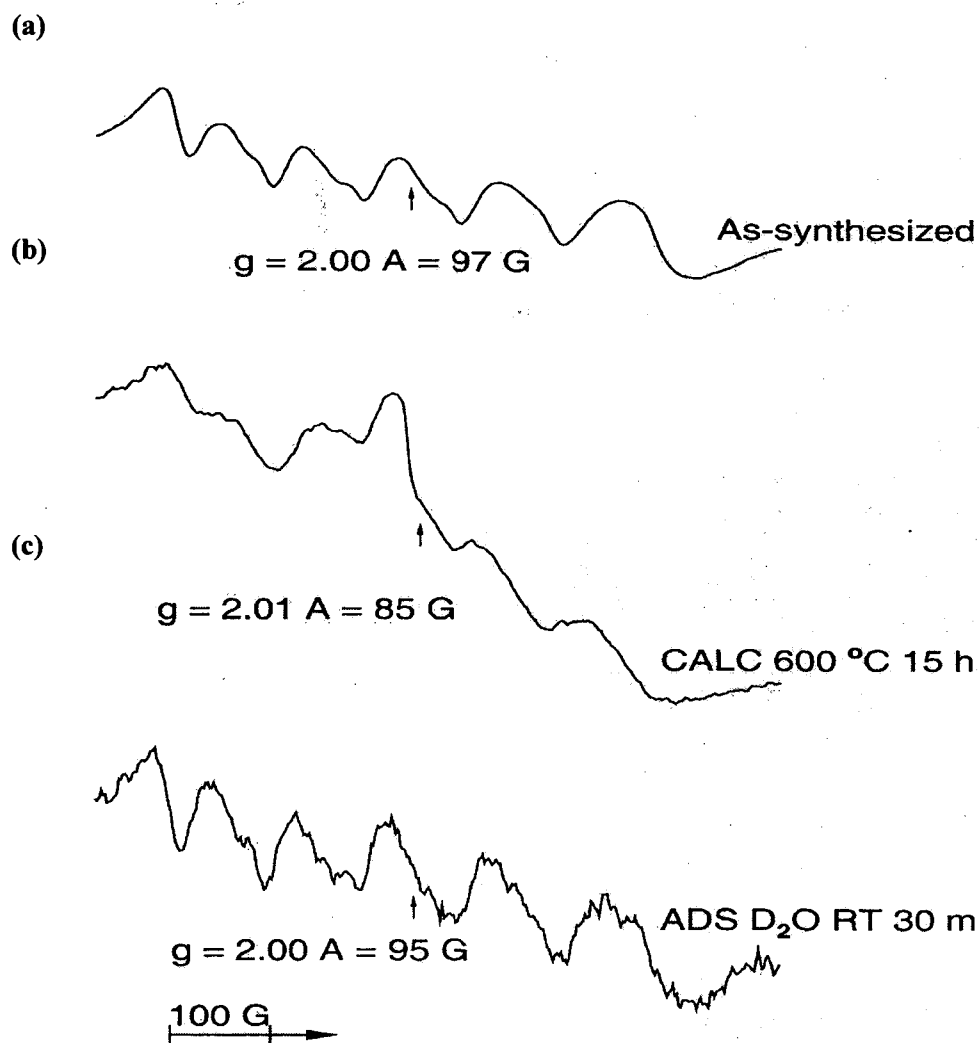


Fig. 6. ESR spectra recorded at 77 K (a) as-synthesized MnH-SAPO-34 with 0.01 mol% manganese and (b) MnH-SAPO-34 with 0.01 mol% manganese calcined at 600 °C for 15 h and (c) calcined MnH-SAPO-34 with 0.01 mol% manganese adsorbed D₂O at room temperature for 30 min.

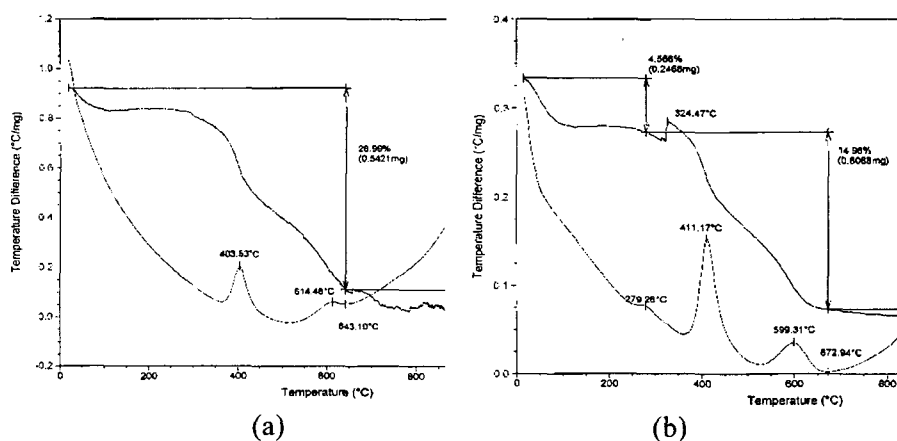


Fig. 7. TGA curves of (a) as-synthesized MnH-SAPO-34 and (b) MnAPSO-34 recorded under air with a heating rate of 10 °C /min.

While the position of the band at 3600 cm^{-1} (ν_1) does not change, the band at 3450 cm^{-1} (ν_2) of MnH-SAPO-34 is shifted about 10 cm^{-1} to lower energy compared to those in MnAPSO-34 and calcined H-SAPO-34. The MnAPSO-34 framework is regarded as a silicoaluminophosphate matrix which contains Mn(II) ions isomorphously substituted for P(V), Al(III), or Si(IV) ions. This substitution can make the formation of new OH groups bridging Mn(II) and another tetrahedral ions in the framework as found in zeolites. IR bands at 3600 and 3450 cm^{-1} have been assigned to $-\text{Si}-\text{OH}-\text{Al}$ -groups in SAPO-34, formed during the isomorphous substitution of Si(IV) for P(V) in a framework position. The observed shift indicates changes in the OH vibration mode, which can be influenced by such factors as the coordination and the hydrated structure. Infrared spectra shows that the position of a band at about 3450 cm^{-1} which is assigned to a hydroxyl group, is shift by about 10 cm^{-1} toward low energy in MnSAPO-11 versus MnH-SAPO-11.⁶

Electron Spin Echo Modulation. The magnitude of the ESE modulation depth is related to the interaction distance R , the number of interacting nuclei N , and the isotropic hyperfine coupling constant A . While the modulation depth for MnAPSO-34 with adsorbed D_2O was about 0.72, that for (L)MnH-SAPO-34 was about 0.62 as shown in Table 2 (see Fig. 9).

This indicates that the local environment of Mn(II) in (L)MnH-SAPO-34 is different from the location of Mn(II) in MnAPSO-34. This is consistent with the finding that the location of Mn(II) in MnSAPO-11 is different to that of Mn(II) in (L)MnH-SAPO-11.⁶

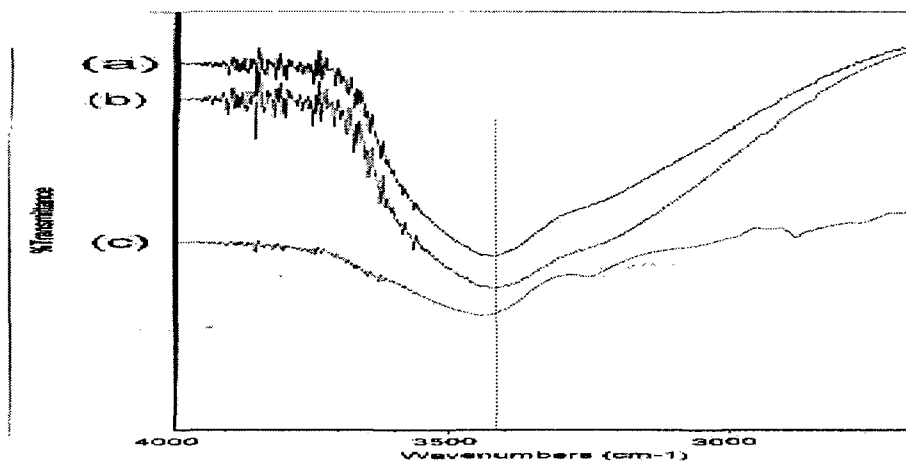


Fig. 8. Infrared spectra of (a) (L) MnH-SAPO-34 and (b) calcined H-SAPO-34 and (c) MnAPSO-34 (0.065 mol%).

The crystal structure of hydrated Mn(II)-exchanged chabazite has been determined by single-crystal diffraction. Mn(II) ions in site I (six-ring window) are found to be a distorted interacting distance and the number of interacting nuclei, we tried to octahedral coordination with three framework oxygen atom and three water.²⁰ The average distance between Mn(II) and the oxygens is approximately 0.23 nm, from which the distance between Mn(II) and the water hydrogens can be calculated to be approximately 0.27 nm. These distances imply the direct coordination of Mn(II) to water. To determine the measured three-pulse ESEM with MnH-SAPO-34 and MnAPSO-34 sample adsorbed D₂O but only the difference in the coordination number was found. The simulation of the three-pulse ESEM data from the MnAPSO-34 sample requires a two-shell model with the following parameter: $N_1 = 2$, $R_1 = 0.26$ nm, $A_1 = 0.14$ MHz, and $N_2 = 2$, $R_2 = 0.36$ nm, $A_2 = 0$ MHz, where N denotes the number of deuterons, R is the distance between Mn(II) and the deuterons, A is the isotropic hyperfine coupling constant, and subscripts 1 and 2 indicate the shell number (see Fig. 10).

This two-shell model agrees well with that from the ESEM simulation of MnAPO-11 with adsorbed D₂O.⁵ Since R_1 is significantly shorter than 0.27 nm, the oxygen end of water cannot coordinate directly with Mn(II). The most likely formed local geometry of Mn(II) is with two waters oriented such that one of the deuterium (D_1) is only 0.25 nm away from the Mn(II) while the outer deuterium (D_2) is 0.36 nm away (see Fig. 11 and Table 3). Such a geometry indicates that Mn(II) is in a negatively charged site, which is the evidence for Mn(II) substituted into a framework site. Previously we found that the distance between ion-exchanged Cu(II) and D for (L)CuH-SAPO-34 with adsorbed D₂O was 0.28

nm.¹³ Fig. 12 and 13 represent the possible geometrical differences of MnH-SAPO-34 and MnAPSO-34. While ion-exchanged Mn(II) ions coordinates three framework oxygen atoms in a six-ring window and three water molecules resulting in a distorted octahedral geometry (Fig. 12), Mn(II) in MnAPSO-34 is located in a tetrahedral framework site and interacts with two deuteriums (D_1) in bond-oriented water (Fig. 13).

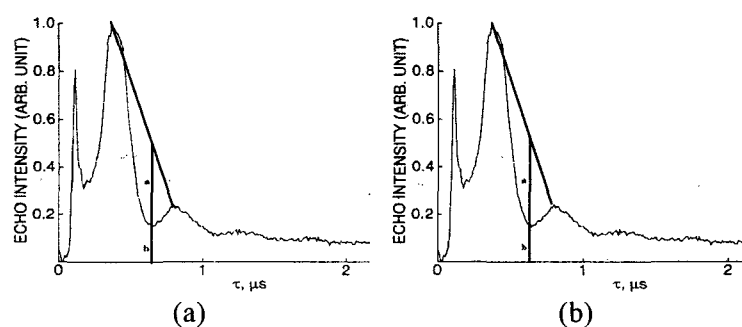


Fig. 9. Two-pulse ESEM recorded at 4 K of (a) MnAPSO-34 with 0.07 mol% manganese with D_2O and (b) MnH-SAPO-34 with 0.07 mol% manganese adsorbed D_2O . The normalized deuterium depths ($a/(a+b)$) are 0.72 and 0.62, respectively.

Table 2. Deuterium Modulation Depth from MnAPSO-34 and MnH-SAPO-34 with Adsorbed D_2O .

Sample	normalized modulation depth
MnAPSO-34	0.72
MnH-SAPO-34	0.62

Table 3. Simulation Parameters of Three-pulse ESEM of Mn(II) in MnAPSO-34 and MnH-SAPO-34 Treated with D_2O .

Sample	shell	N	R(nm)	A MHz
MnAPSO-34 ^a	2	2	0.25	0.14
		2	0.36	0
MnH-SAPO-34 ^a	2	4	0.27	0.14
		2	0.36	0
MnAPSO-34 ^b	2	1	0.26	0.14
		2	0.36	0.15
MnH-SAPO-34 ^b	1	6	0.28	0.20

a : 0.07 mol%, b : 0.01 mol%

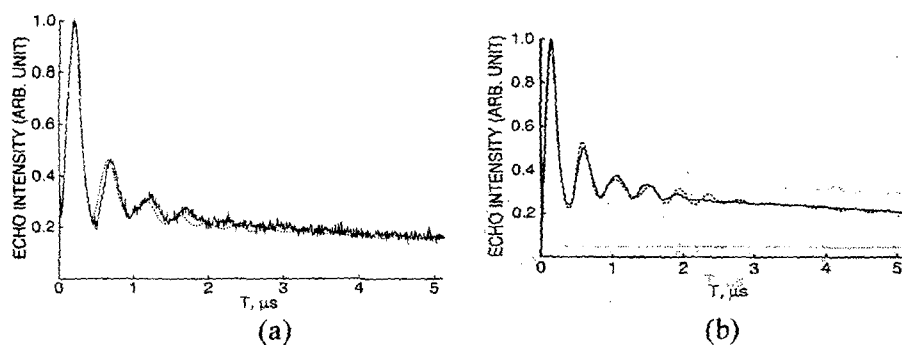


Fig. 10. Experimental and simulated (dashed line) three-pulse ESEM at 4 K 0.01 mol% MnAPSO-34 (a) [$N_1 = 2$ at $R_1 = 0.26 \pm 0.01$ nm, $A_1 = 0.14$ MHz and $N_2 = 2$ at $R_2 = 0.36$ nm, $A_2 = 0$ MHz], MnH-SAPO-34 (b) [$N_1 = 6$ at $R_1 = 0.28$ nm, $A_1 = 0.2$ MHz].

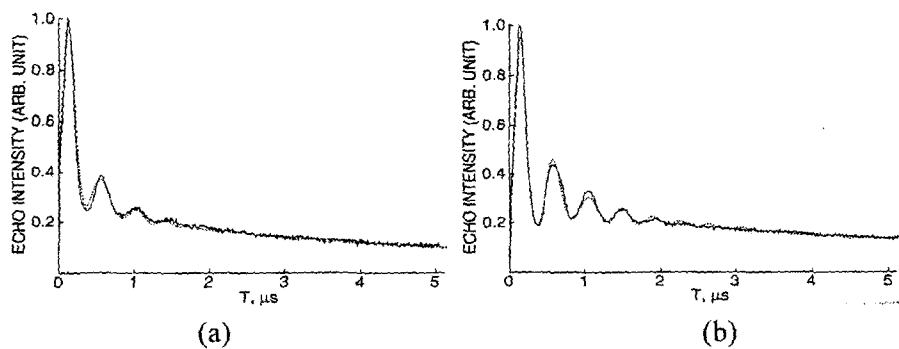


Fig. 11. Experimental and simulated (dashed line) three-pulse ESEM at 4 K 0.065 mol% MnAPSO-34 (a) [$N_1 = 2$ at $R_1 = 0.25 \pm 0.01$ nm, $A_1 = 0.14$ MHz and $N_2 = 2$ at $R_2 = 0.36$ nm, $A_2 = 0$ MHz], MnH-SAPO-34 (b) [$N_1 = 4$ at $R_1 = 0.27$ nm, $A_1 = 0.14$ MHz, $N_2 = 2$ at $R_2 = 0.36$ nm, $A_2 = 0$ MHz].

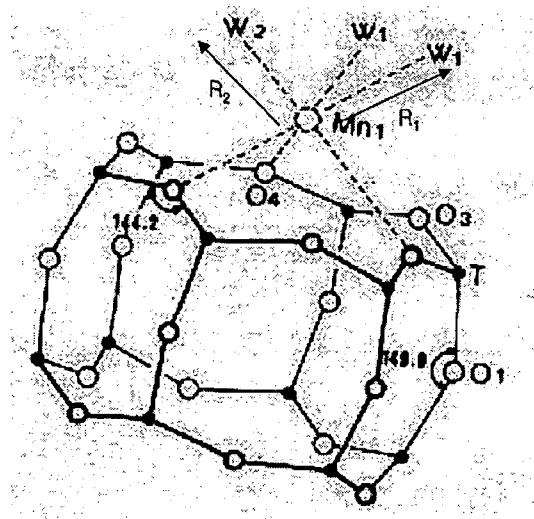


Fig. 12. A view of six-ring window in MnH-SAPO-34 ($R_1 = 0.27$ nm, $R_2 = 0.36$ nm, $W = D_2O$)

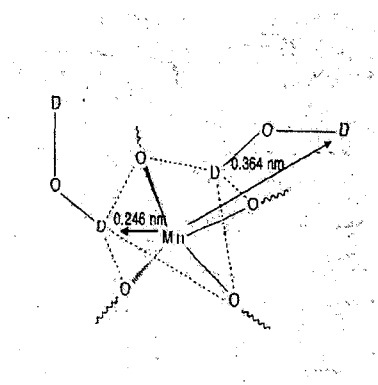


Fig. 13. Proposed schematic diagram for Mn- D_2O interaction of MnAPSO-34. Where Mn is located in the framework.

CONCLUSIONS

This work shows the spectroscopic evidence that Mn(II) is in a framework position in synthesized MnAPSO-34, by comparison with ion-exchanged MnH-SAPO-34 samples in which Mn(II) is in an extraframework position. At low Mn(II) content Mn(II) was substituted into a framework position of MnAPSO-34. The local environment of Mn(II) in MnAPSO-34 which is different from that in the ion-exchanged (L)MnH-SAPO-34 sample can be induced from the pale violet color of calcined MnAPSO-34, the higher decomposition temperature of the templating agent for as-synthesized MnAPSO-34, the shift of the OH vibration frequency toward lower energy for MnH-SAPO-34, and the deeper two-pulse ESE modulation depth of for MnAPSO-34. More direct evidence was found from three-pulse ESEM simulations of adsorbate structure for MnAPSO-34 with adsorbed D₂O.

Acknowledgements

This research financially supported by the Changwon National University in 2002. The authors are also grateful to Prof. Larry Kevan at the Department of Chemistry in University of Houston for ESEM measurements

REFERENCES

1. S. T. Wilson, B. M. Lok, C. A. Messina, T. R. Cannan and E. M. Flanigen, *J. Am. Chem. Soc.*, **104**, 1146 (1982).
2. B. M. Lok, C. A. Messina, R. L. Patton, R. T. Gajek, T. R. Cannan and E. M. Flanigen, *J. Am. Chem. Soc.*, **106**, 6092 (1984).
3. R. Szostak, *Molecular Sieves ; Principle of Synthesis and Identification*, Van Nostrand Reinhold ; NewYork, 1989 Chap 4.
4. (a) B. M. Lok, C. A. Messina, R. L. Patton, R. T. Gajek, T. R. Cannan and E. M. Flanigen, *U. S. Pat.* 4400871, (1984) (b) B. M. Lok, C. A. Messina, R. L. Patton, R. T. Gajek, T. R. Cannan and E. M. Flanigen, *J. Am. Chem. Soc.*, **106**, 6092 (1984).
5. G. Brouet, X. Chen, C. W. Lee and L. Kevan, *J. Am. Chem. Soc.*, **114**, 3720 (1992).
6. C. W. Lee, X. Chen, G. Brouet and L. Kevan, *J. Phys. Chem.* **96**, 3110 (1992).
7. D. Goldfarb, *Zeolites*, **9**, 509 (1989).
8. Z. Lev, A. M. Raitsimring and D. Goldfarb, *J. Phys. Chem.* **95**, 7830 (1991).
9. Y. Xu, J. W. Couves, R. H. Jones, C. R. A. Catlow, G. N. Greaves, J. Chen, and J. M. Thomas, *J. Phys. Chem. Solids* **52**, 1229 (1991).
10. B. Kraushaar-Czarnetzki, W. G. M. Hoogervorst, R. R. Andrea, C. A. Emeis, W. H. J. Stork, in *Zeolite Chemistry and Catalysis*; P. A. Jacobs, N. I. Jaeger, L. Kubelkora and B. Wichterlov; Elsevier; Amsterdam pp231-240 (1991).

11. L. E. Iton, I. Choi, J. A. Desjardins and V. A. Maroni, *Zeolites*, **9**, 535 (1989).
12. Y. Xu, P. J. Maddox and J. W. Couves, *J. Chem. Soc., Faraday Tras.*, **86**, 425 (1990).
13. M. Zamadics, X. Chen, and L. Kevan, *J. Phys. Chem.* **96**, 2692 (1992).
14. L. Kevan, in *Time domain Electron Spin Resonance*; Wiley Interscience, New York, pp279-341 (1979).
15. S. A. Dikanov, A. A. Shubin and V. N. Parmon, *J. Magn. Reson.* **42**, 474 (1981).
16. G. Brouet, X. Chen, C. W. Lee and L. Kevan, *J. Am. Chem. Soc.*, **114**, 3720 (1992).
17. Z. Levi, D. Goldfarb and J. Batisto, *J. Am. Chem.Soc.*, submitted.
18. A. M. Prakash and Unnikrishnan, *J. Chem. Soc. Faraday Trans.* **90**(15) 2291 (1994).
19. Ward, J. W. in *Zeolite Chemistry and Catalysis*; Rabo, J., Ed.; ACS. Monograph 171; American Chemical Society; Washington, DC, 1996, p118.
20. M. Calligaris, A. Mezzetti, G. Mardin and L. Randaccino, *Zeolites*, **5**, 317 (1985).